第 35 卷第 3 期
2019 年 3 月

无 机 化 学 学 报
CHINESE JOURNAL OF INORGANIC CHEMISTRY

Vol.35 No.3
537-545

锂离子电池负极硅–热解碳–石墨复合材料的制备及性能

杨学兵* 张林伟
(江西省科学院应用物理研究所,南昌 330029)

摘要:以沥青为碳前驱物,通过加热分解法制备了具有不同热解碳含量的硅–热解碳–石墨复合材料,并测试及分析了材料的形貌、结构及电化学性能。结果表明,沥青质量在 320~560 ℃的温度区间内迅速减小,沥青质量的减小是由于氢元素的去除。经过高温分解制得的热解碳与沥青的质量比率为 65%。在硅–热解碳–石墨复合材料中,硅颗粒分散在石墨表面,热解碳覆盖在硅颗粒表面,热解碳增强了硅颗粒与石墨间的界面结合力。适当含量的热解碳增大了复合材料的放电比容量且改善了循环稳定性;过量的热解碳不能进一步提升复合材料的放电容量。

关键词:锂离子电池;负极材料;硅;石墨
中图分类号:O646 **文献标识码**:A **文章编号**:1001-4861(2019)03-0537-09
DOI:10.11862/CJIC.2019.063

Preparation and Performance of Silicon-Pyrolytic Carbon-Graphite Composite as Anode Material for Lithium-Ion Batteries

YANG Xue-Bing* ZHANG Lin-Wei
(*Institute of Applied Physics, Jiangxi Academy of Science, Nanchang* 330029, *China*)

Abstract: Silicon-pyrolytic carbon-graphite composite with different content of pyrolytic carbon has been synthesized through pyrolysis. Pitch has been used as precursor of pyrolytic carbon. Morphology, structure and electrochemical performance of materials have been tested and analyzed. The results showed that the mass of pitch decreased rapidly from 320 to 560 ℃. The decrease of mass results from removal of hydrogen in pitch. Mass ratio between pyrolytic carbon and pitch was about 65% through pyrolysis process. In silicon-pyrolytic carbon-graphite composite, silicon particles were dispersed on the surface of graphite. Pyrolytic carbon covered silicon particles, and enhanced the interface adhesion between silicon particles and graphite. Appropriate content of pyrolytic carbon could increase the discharge capacity and improve the cycle stability of composite while excessive content of pyrolytic carbon could not further enhance discharge capacity.

Keywords: lithium-ion batteries; anode material; silicon; graphite

Development of portable electronic devices and electrical vehicles requires high energy density of batteries. The use of electrode materials with high specific capacity can increase the energy density of lithium-ion batteries. Graphite is the most common anode material in commercial lithium-ion batteries. Theoretical specific capacity of graphite is 372 mAh·g^{-1} [1]. Silicon is another kind of anode material for lithium-ion batteries with theoretical specific capacity of 4 200 mAh·g^{-1} when the reaction product between silicon and lithium is $Li_{22}Si_4$[2]. In comparison with graphite, theoretical specific capacity of silicon is

收稿日期:2018-10-10。收修改稿日期:2018-12-19。
国家青年科学基金项目(No.51701089)和江西省重点研发计划项目(No.20161BBH80061)资助。
*通信联系人。E-mail:xbyjz@163.com

higher and the operating potential of silicon is lower. Thus, silicon is a promising anode material for lithium-ion batteries[3-5].

However, cycle discharge stability of silicon electrodes is low. The main reason for the problem is the volume change of silicon during discharge and charge. During discharge, the volume expansion of silicon is about 300%[6]. The volume change of silicon destroys the inter-particle electric contact. Besides, the volume change breaks the solid-electrolyte interface film and exposes the fresh interface[7]. The fresh interface consumes electrolyte and new solid-electrolyte interface film forms. Breakage and formation of solid-electrolyte interface film makes the film thick. Thick interface film lowers the electrochemical activity of silicon and reduces the discharge capacity.

Strategies have been developed to improve the electrochemical performance of silicon anodes. One strategy is the fabrication of silicon material with nano-structure such as hollow nano-spheres and nanotubes[8]. Hollow silicon nano-spheres and silicon nanotubes have large void space which accommodates the volume change of silicon in processes of discharge and charge. Another strategy is preparation of electrically conductive coatings[9-13]. Carbon coating and electrically conductive polymer coatings increase the electric conductivity of silicon and buffer the volume change of silicon.

The reports indicate that it is important to increase the electric conductivity of silicon and buffer the volume change of silicon. In this paper, pyrolytic carbon from pitch has been used to increase the electric conductivity of silicon and improve the adhesion between silicon and graphite. Silicon-pyrolytic carbon-graphite composite with different content of pyrolytic carbon has been synthesized through pyrolysis.

1 Experimental

1.1 Preparation and characterization of silicon-pyrolytic carbon-graphite composite

Silicon-pyrolytic carbon-graphite composite was synthesized by heating the mixture of silicon, pitch and graphite. Pitch was the carbon precursor used to fabricate pyrolytic carbon. Silicon (Shuitian ST-NANO Science & Technology Co., Ltd., Shanghai, China), pitch and graphite (10 μm, Tianhe Graphite Co., Ltd., Qingdao, China) were mixed by milling in mass ratios of 1∶0.5∶7 and 1∶1∶7 respectively. After the mixture was dried at 70 ℃ for 2 h, the mixture was heated at 900 ℃ for 2 h in the atmosphere of nitrogen gas. The product was silicon-pyrolytic carbon-graphite composite. Silicon-pyrolytic carbon-graphite composite-1 and silicon-pyrolytic carbon-graphite composite-2 correspond to the mass ratios of 1∶0.5∶7 and 1∶1∶7 respectively. Silicon-graphite composite was synthesized by milling mixture of silicon and graphite in mass ratio of 1∶7.

Morphology and element composition of materials were tested by scanning electron microscopy (SEM) with operation voltage of 15 kV. Crystal structure of materials was analyzed by X-ray diffraction (XRD, Cu $K\alpha$ radiation (λ=0.154 06 nm, U=40 kV, I=30 mA)) in the 2θ range of 10°~90°. Chemical bonds of materials were analyzed through infrared spectra and Raman spectra. Thermo-gravimetric (TG) analysis was carried out by TG instrument in the atmosphere of nitrogen.

1.2 Fabrication of silicon-pyrolytic carbon-graphite electrodes and assembly of coin cells

The electrodes were fabricated by mixing active materials, electrically conductive substance and binder in mass ratio of 8∶1∶1. The binder was LA133 (15% (*w*/*w*), Chengdu Indigo power sources Co., Ltd., Chengdu, China). LA133 was dissolved in water at first. Then silicon-pyrolytic carbon-graphite composite and conductive carbon were added to the solution. After stirring, the slurry was spread over the surface of copper foil. Subsequently, the copper foil was dried under vacuum at 80 ℃ for 12 h. Finally, the copper foil was punched to obtain circular electrodes with diameter of 12 mm. Silicon-graphite composite electrodes were fabricated according to the above method.

Coin cells (CR2016) were assembled in glove box (MIKROUNA) filled with purified argon gas. Lithium metal foils were used as counter electrodes to silicon-

pyrolytic carbon-graphite electrodes. Separator between the two kinds of electrodes was polypropylene microporous film (Celgard 2400). Cyclic voltammetry tests were carried out through electrochemical work station (Ivium Technologies). Discharge and charge capacity of coin cells were obtained through battery test system (Neware, Shenzhen, China). The rate of discharge and charge was 0.1C and the potential range was from 0.005 to 1.2 V. Theoretical capacity of composite was based on the content of components. Calculated theoretical capacity of silicon, graphite and pyrolytic carbon were 3 500, 350 and 300 $mAh \cdot g^{-1}$ respectively.

2 Results and discussion

The SEM images of graphite and silicon are presented in Fig.1. Graphite was composed of particles with irregular shape (Fig.1(a)). Particle size of graphite was about 10 μm. Silicon was composed of tiny particles with the diameter below 500 nm, and the particle size was close in Fig.1(b).

SEM images of silicon-graphite composite, silicon-pyrolytic carbon-graphite composite-1 and silicon-pyrolytic carbon-graphite composite-2 are presented in Fig.2. Silicon particles were dispersed although few silicon particles was on the surface of graphite flakes in Fig.2(a). Silicon particles of silicon-pyrolytic carbon-graphite composite-1 were dispersed on the surface of graphite in Fig.2(b). Pyrolytic carbon from pitch was not obvious in the figure as it was amorphous. In Fig. 2(c), morphology of silicon particles was similar to that in Fig.2(b). The increase of the content of pyrolytic carbon from pitch has not obviously changed the

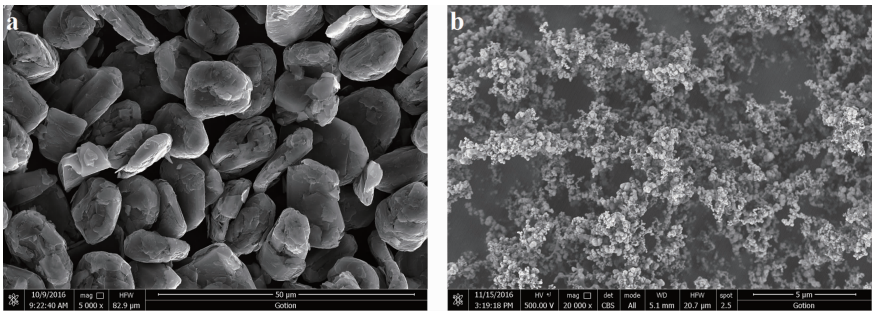

Fig.1　SEM images of graphite (a) and silicon (b)

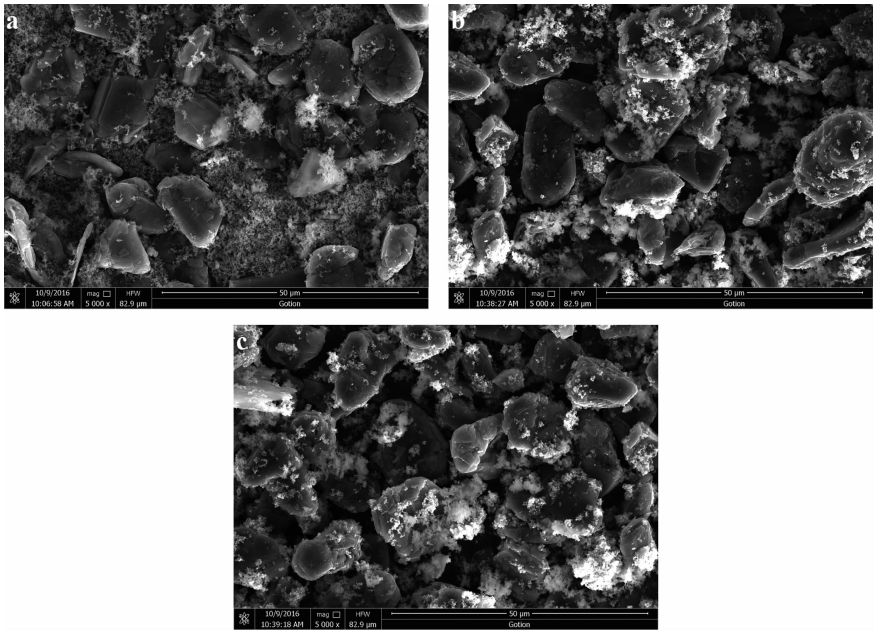

Fig.2　SEM images of silicon-graphite composite (a), silicon-pyrolytic carbon-graphite composite-1 (b) and silicon-pyrolytic carbon-graphite composite-2 (c)

morphology of silicon particles.

Fig.3 presents the XRD patterns of graphite, silicon, pitch, pyrolytic carbon, silicon-graphite composite, silicon-pyrolytic carbon-graphite composite-1 and silicon-pyrolytic carbon-graphite composite-2. In the XRD pattern of graphite, the diffraction peak at about 26.6° corresponded to (002) crystal plane (PDF No.65-6212). This sharp diffraction peak indicated that the crystallization degree of graphite was high. The other diffraction peaks at 44.2° and 54.5° were ascribed to (101) and (004) crystal planes respectively. In the XRD pattern of silicon, there were several sharp diffraction peaks which demonstrated that the high crystallization degree of silicon. The highest diffraction peak was at about 28.4° corresponding to the (111) crystal plane (PDF No.27-1402)[14]. The broad diffraction peak of pitch at about 24.4° is ascribed to the low crystallization degree of pitch. The intensity of diffraction peaks of pyrolytic carbon at about 25.3° was stronger than that of pitch, which demonstrated the higher crystallization degree of pyrolytic carbon. The diffraction peaks of graphite and silicon existed in XRD pattern of silicon-graphite composite, and the intensity of diffraction peaks of silicon was lower than that of graphite. The low relative intensity showes the low content of silicon in silicon-graphite composite. The diffraction peaks of pyrolytic carbon were not obvious in the XRD patterns of silicon-pyrolytic carbon-graphite composite-1 and silicon-pyrolytic carbon-graphite composite-2.

Fig.4 shows the Raman spectra of the materials. In the Raman spectrum of graphite, the D-band was at about 1 346 cm^{-1} and the G-band was at about 1 573 cm^{-1} [15-16]. The D-band was linked with disorder in

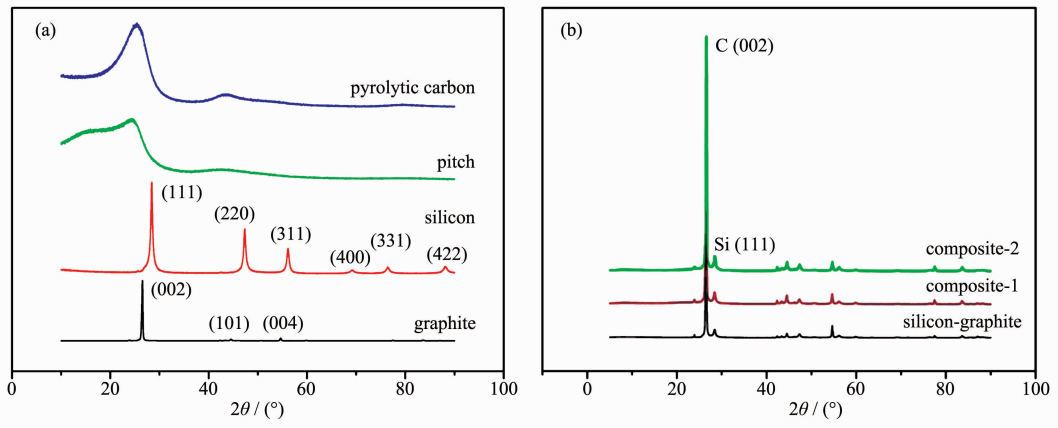

Fig.3 XRD patterns of graphite, silicon, pitch, pyrolytic carbon, silicon-graphite composite, silicon-pyrolytic carbon-graphite composite-1 and silicon-pyrolytic carbon-graphite composite-2

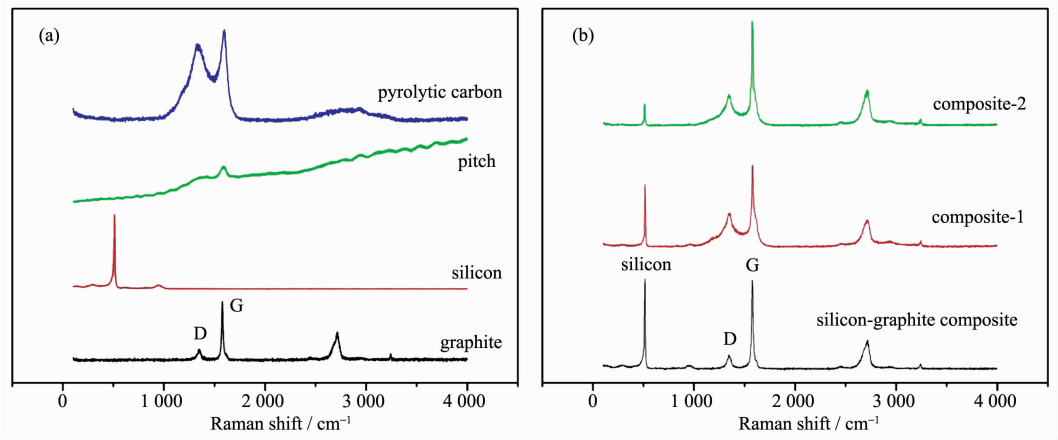

Fig.4 Raman spectra of graphite, silicon, pitch, pyrolytic carbon, silicon-graphite composite, silicon-pyrolytic carbon-graphite composite-1 and silicon-pyrolytic carbon-graphite composite-2

carbon structure and the G-band was ascribed to vibration of carbon atoms with sp^2 bonds[17-18]. The high relative intensity of G-band demonstrated the high graphitization degree of graphite. The peak at about 514 cm^{-1} was belonged to silicon in the Raman spectrum of silicon. The Raman bands of pitch were not obvious. The D-band and G-band of pyrolytic carbon were at about 1 329 and 1 599 cm^{-1} respectively. In comparison with pitch, Raman bands of pyrolytic carbon were apparent, which results from the carbonization of pitch through pyrolysis process. Relative intensity for G-band of pyrolytic carbon was lower than that of graphite. The result indicated that graphitization degree of pyrolytic carbon is lower than that of graphite. The D-band and G-band existed in the Raman spectra of silicon-graphite composite. The relative intensity for G-band was relatively high. The Raman band of silicon, D-band and G-band were appared in the Raman spectra of silicon-pyrolytic carbon-graphite composite-1 and silicon-pyrolytic carbon-graphite composite-2. The D-band and G-band are produced by pyrolytic carbon and graphite.

Fig.5 shows the FT-IR spectra of the materials. In the FT-IR spectrum of graphite, there were two absorption bands at about 1 637 and 3 445 cm^{-1} respectively. The two absorption bands correspond to the vibration of hydrogen-oxygen bonds in adsorbed water[19]. FT-IR spectrum of silicon was similar to that of graphite. There was an absorption band at about 742 cm^{-1} in the FT-IR spectrum of pitch which was linked with vibration of carbon-hydrogen bonds[20]. The result demonstrated the existence of hydrogen element in pitch. The absorption band of carbon-hydrogen bonds disappeared in the FT-IR spectrum of pyrolytic carbon. The disappearance of absorption band results from the removal of hydrogen through pyrolysis process. FT-IR spectrum of silicon-graphite composite was similar to that of silicon. There was not obvious difference between the FT-IR spectrum of silicon-pyrolytic carbon-graphite composite-1 and that of silicon-pyrolytic carbon-graphite composite-2. The increase in content of pyrolytic carbon does not obviously change the FT-IR spectrum.

Thermo-gravimetric curve of pitch is presented in Fig.6. When the temperature was below 320 ℃, the mass of pitch was nearly unchanged. As the temperature increased from 320 to 560 ℃, the mass of pitch decreased rapidly. The decrease of mass results from removal of hydrogen in pitch. With the increase of temperature, the mass of pitch keeps relatively stable. The mass maintained stable after the complete decomposition of pitch. The stable mass rate was about 65% through the pyrolysis process.

Fig.7 presents SEM image, EDS mappings and TEM image of silicon-pyrolytic carbon composite-1. The element distribution of those silicon particles in Fig.7a are showed in the EDS mappings (Fig.7(b,c)). It can be seen that the distribution of carbon was similar to that of silicon which indicated that pyrolytic carbon exists on the surface of silicon particles. In Fig.7(d), it

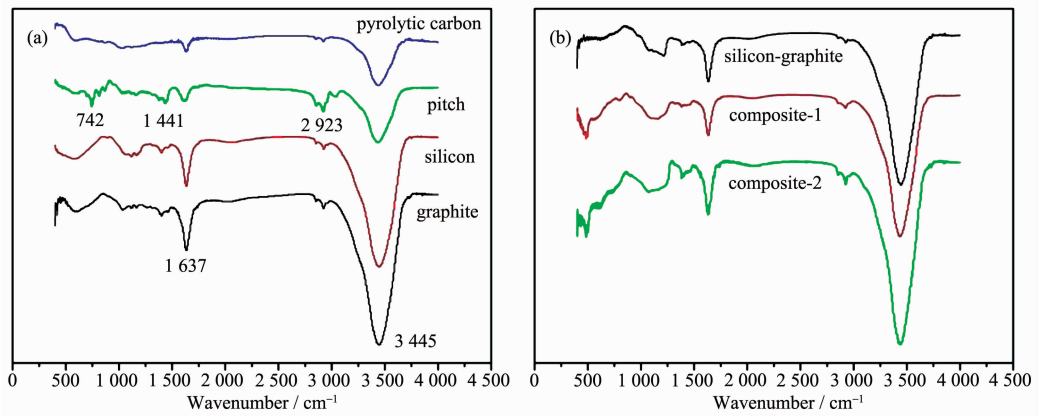

Fig.5　FT-IR spectra of graphite, silicon pitch, pyrolytic carbon, silicon-graphite composite, silicon-pyrolytic carbon-graphite composite-1 and silicon-pyrolytic carbon-graphite composite-2

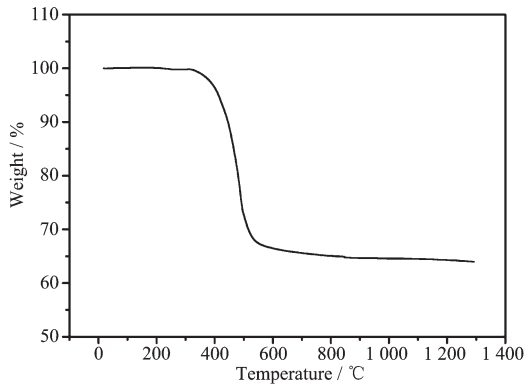

Fig.6 Thermo-gravimetric curve of pitch

can be seen that silicon particles were wrapped by pyrolytic carbon.

Fig.8 shows the discharge and charge curves of silicon-graphite composite, silicon-pyrolytic carbon-graphite composite-1 and silicon-pyrolytic carbon-graphite composite-2 electrode. In the first cycle of silicon-graphite composite electrode, the discharge capacity, the charge capacity and the initial coulombic efficiency was about 660, 527 mAh·g^{-1} and 79.8%, respectively. In the second cycle of silicon-graphite composite, discharge and charge capacity were lower than those of the first cycle. The reason is that a part of lithium ions existed in the solid interface film on silicon-graphite electrode. The discharge voltage in the second cycle was higher than that in the first cycle because of the activation of silicon-graphite composite electrode. The discharge and charge capacity decreased with the increase of cycle number, whereas the potential of discharge and charge was close. Fig.8(b) presents the discharge and charge curves of silicon-pyrolytic carbon-graphite composite-1 electrode. In the first cycle, discharge capacity and charge capacity were 706 and 570 mAh·g^{-1} respectively. The discharge capacity and charge capacity were higher than those of silicon-graphite composite electrode, which results from higher electric conductivity for silicon particles in silicon-pyrolytic carbon-graphite composite-1 electrode. The initial coulombic efficiency was 80.7%. When the cycle number increased, the potential of discharge and charge was close. Fig.8(c) shows the discharge and charge curves of silicon-pyrolytic carbon-graphite composite-2 electrode. In the first cycle, discharge and charge capacity are 685 and 541 mAh·g^{-1}, respectively. The discharge and charge capacity were lower than those of silicon-pyrolytic carbon-graphite composite-1 electrode. The increase of the content of pyrolytic carbon results in the decrease of discharge and charge capacity. Excessive pyrolytic carbon does

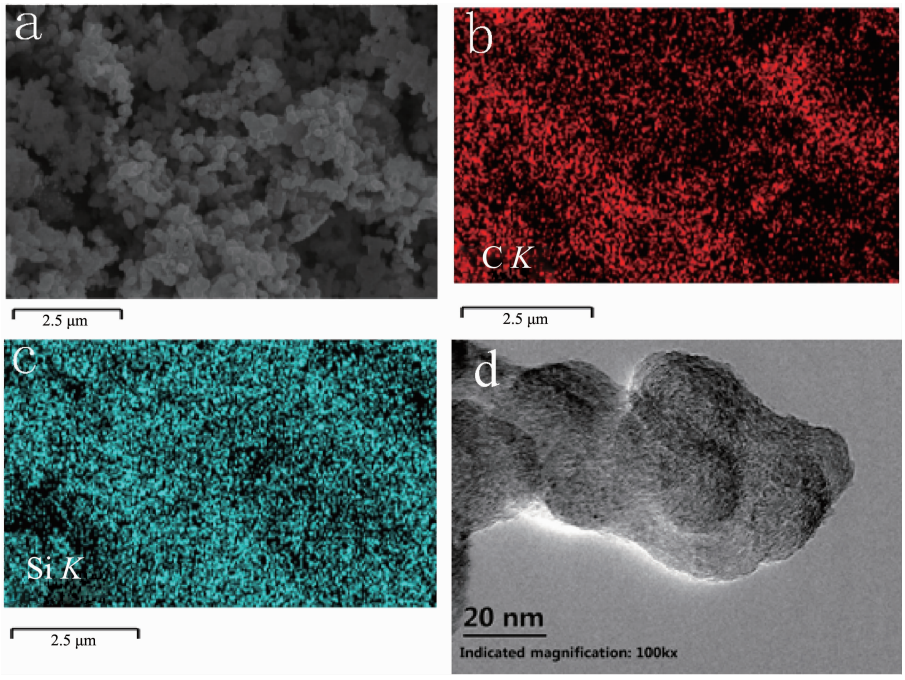

Fig.7 SEM image (a), EDS mappings (b, c) and TEM image (d) of silicon-pyrolytic carbon-graphite composite-1

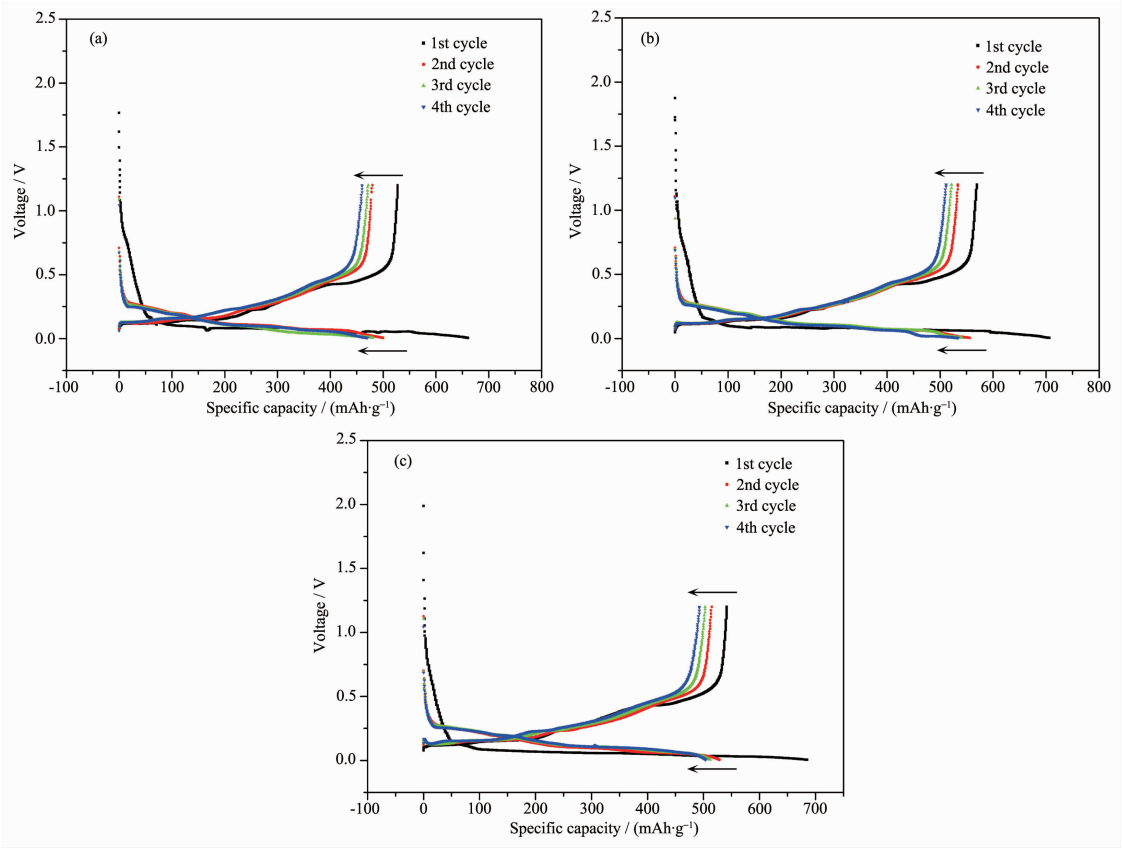

Fig.8　Discharge and charge curves of silicon-graphite composite (a), silicon-pyrolytic carbon-graphite composite-1 (b) and silicon-pyrolytic carbon-graphite composite-2 (c) electrode

not obviously increase the electric conductivity of silicon particles.

Cyclic voltammetry curves of the three kinds of composite electrode are shown in Fig.9. In Fig.9 (a), the reduction peak at ~0 V corresponds to lithiation of silicon and graphite. The intensity of reduction peak above 0 V increased with the increase of the cycle number, which results from activation of silicon-graphite composite electrode[21-22]. The activation of electrode is also verified in Fig.8. The reduction peaks above 0 V in Fig.9(b) were linked with lithiation of amorphous silicon[23]. The reduction peaks were more obvious than those of silicon-graphite composite because the pyrolytic carbon covering on silicon particles enhances the electric conductivity of silicon particles. In Fig.9(c), reduction peaks of silicon-pyrolytic carbon-graphite composite-2 electrode were similar to those of silicon-pyrolytic carbon-graphite composite-1 in Fig.9(b).

Fig.10 shows the cycle performance of the electrodes. The initial discharge and the second discharge capacity of silicon-graphite composite electrode were 660 and 500 mAh·g^{-1} respectively. The discharge capacity decreases rapidly with the increase of the cycle number because of the big volume change of silicon particles. The big volume change leads to breakage of solid electrolyte interface film and formation of new solid electrolyte interface film which consumed the lithium ions. The discharge capacity of silicon-pyrolytic carbon-graphite composite-1 electrode was higher than that of silicon-graphite composite electrode. Pyrolytic carbon increases the electric conductivity of silicon particles and enhances the electrochemical activity. Besides, the cycle stability of silicon-pyrolytic carbon-graphite composite-1 electrode is better than that of silicon-graphite composite electrode in Fig.10. The improvement of cycle stability is ascribed to the strong interface adhesion between silicon particles and graphite through pyrolytic carbon[4]. Volume change of silicon

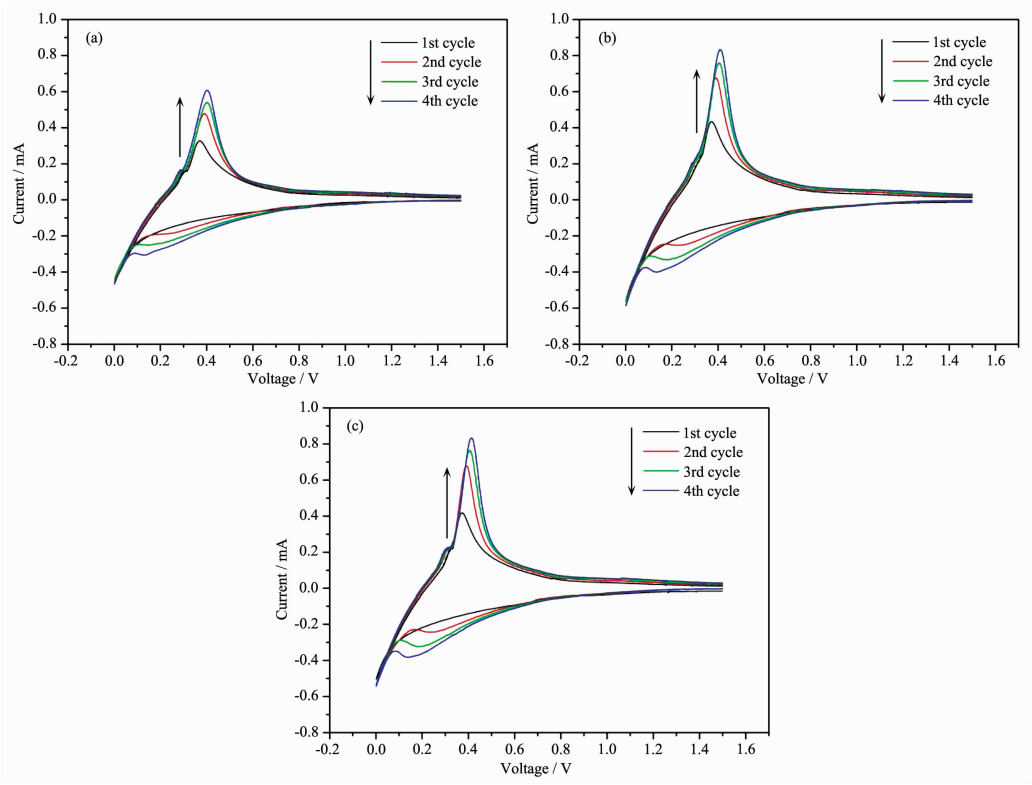

Fig.9 Cyclic voltammetry curves of silicon-graphite composite (a), silicon-pyrolytic carbon-graphite composite-1 (b) and silicon-pyrolytic carbon-graphite composite-2 (c) electrode

particles was effectively relieved by graphite through the strong interface adhesion. The discharge capacity of silicon-pyrolytic carbon-graphite composite-2 composite electrode was lower than that of silicon-pyrolytic carbon-graphite composite-1 electrode. As the content of pyrolytic carbon increased, the electric conductivity of silicon particles could not be further enhanced. At the same time, the discharge capacity of pyrolytic carbon was relatively low.

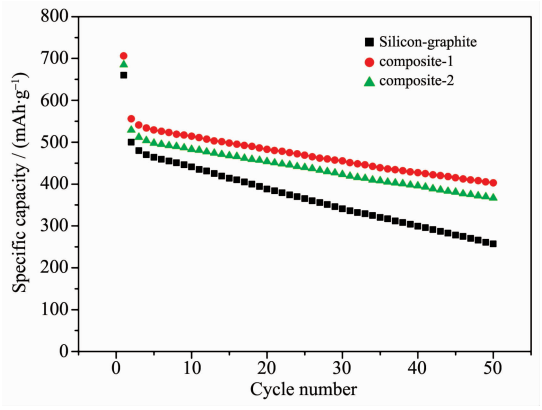

Fig.10 Cycle performance of silicon-graphite composite, silicon-pyrolytic carbon-graphite composite-1 and silicon-pyrolytic carbon-graphite composite-2 electrode

3 Conclusions

In pyrolytic process, the mass of pitch decreased rapidly in temperature range from 320 to 560 ℃. The decrease of mass results from removal of hydrogen in pitch. The mass ratio between pyrolytic carbon and pitch was about 65% . The silicon particles were dispersed on the surface of graphite. Pyrolytic carbon covered the silicon particles in silicon-pyrolytic carbon-graphite composite that increases the electric conductivity of silicon particles and enhances the interface adhesion between silicon particles and graphite. The appropriate content of pyrolytic carbon increases the discharge capacity and improves cycle stability of composite and the excessive content of pyrolytic carbon does not further enhance discharge capacity. The improvement of cycle stability is ascribed to the strong interface adhesion between silicon particles and graphite. The volume change of silicon particles is effectively relieved by graphite through the strong interface adhesion.

References:

[1] Fuchsbichler B, Stangl C, Kren H, et al. *J. Power Sources*, **2011**,**196**:2889-2892

[2] Liu J, Kopold P, Aken P A V, et al. *Angew. Chem. Int. Ed*, **2015**,**127**:9768-9772

[3] TerranovaM L, Orlanducci S, Tamburri E, et al. *J. Power Sources*, **2014**,**246**:167-177

[4] Su M R, Wang Z X, Guo H J, et al. *Electrochim. Acta*, **2014**,**116**:230-236

[5] Li B B, Gao X F, Li J Y, et al. *Environ. Sci. Technol.*, **2014**, **48**:3047-3055

[6] Ge M Y, Rong J P, Fang X, et al. *Nano Lett.*, **2012**,**12**:2318-2323

[7] Lin D C, Lu Z D, Hsu P C, et al. *Energy Environ. Sci.*, **2015**,**8**:2371-2376

[8] Wu H, Chan G, Choi J W, et al. *Nat. Nanotechnol.*, **2012**,**7**: 310-315

[9] Zhang R Y, Du Y J, Li D, et al. *Adv. Mater.*, **2014**,**26**(39): 6749-6755

[10]Wu H, Yu G H, Pan L J, et al. *Nat. Commun.*, **2013**,**4**(3): 1943-1948

[11]Ji J Y, Ji H X, Zhang L L, et al. *Adv. Mater.*, **2013**,**25**(33): 4673-4677

[12]Chang J B, Huang X K, Zhou G H, et al. *Adv. Mater.*, **2014**, **26**(5):758-764

[13]Wang C, Wu H, Chen Z, et al. *Nat. Chem.*, **2013**,**5**(12):1042-1048

[14]CAI Jian-Xin(蔡建信), LI Zhi-Peng(李志鹏), LI Wei(李巍), et al. *Chinese J. Inorg. Chem.*(无机化学学报), **2017**,**33**(10): 1763-1768

[15]Ju Z C, Wang T T, Wang L C, et al. *Carbon*, **2010**,**48**(12): 3420-3426

[16]ZHANG Xing-Shuai(张兴帅), XU Xiao-Mu(许笑目), GUO Yu-Zhong(郭玉忠), et al. *Chinese J. Inorg. Chem.*(无机化学学报), **2017**,**33**(3):377-382

[17]ZHANG Ye-Qiong(张业琼), CONG Ye(丛野), ZHANG Jing(张静), et al. *Chinese J. Inorg. Chem.*(无机化学学报), **2018**, **34**(8):1430-1436

[18]Rui X, Sim D, Wong K, et al. *J. Power Sources*, **2012**,**214**: 171-177

[19]LI Juan(李娟), ZHAO An-Ting(赵安婷), SHAO Jiao-Jing(邵娇婧), et al. *Chinese J. Inorg. Chem.*(无机化学学报), **2017**, **33**(7):1231-1235

[20]YANG Yu-Lin(杨昱霖), GAO Ming(高铭), LIANG Jing-Shuang(梁静爽), et al. *Chinese J. Inorg. Chem.*(无机化学学报), **2017**,**33**(12):2262-2270

[21]Lin N, Han Y, Wang L B, et al. *Angew. Chem. Int. Ed.*, **2015**, **54**(12):3822-3825

[22]Wong D P, Suriyaprabha R, Yuvakumar R, et al. *J. Mater. Chem. A*, **2014**,**2**(33):13437-13441

[23]Li J, Dahn J R. *J. Electrochem. Soc.*, **2007**,**154**(3):A156-A161